Enthalpic interaction in block copolymer/homopolymer blend systems: morphological studies of solvent-cast films

Masaya Akiyama
Central Institute, Mitsui Toatsu Chemicals Inc., Yokohama, Japan

and Alex M. Jamieson
Department of Macromolecular Science, Case Western Reserve University, Cleveland, Ohio 44106, USA
(Received 26 July 1991; accepted 23 September 1991)

We report morphological studies of solvent-cast polymer blend films containing a polystyrene/poly(methyl methacrylate) (PS/PMMA) block copolymer with polymers that are miscible with one block copolymer segment, viz. polystyrene (PS), random styrene/acrylonitrile copolymers (SAN) and poly(methyl methacrylate) (PMMA). By utilizing SANs that have four different acrylonitrile (AN) contents, we vary the enthalpic interaction between the SAN copolymer and the block copolymer segments. With polystyrene as the minor constituent, and for a given overall composition ratio and specified molecular weights of the blend components, the morphology of the blends was found to change systematically from dispersed spheres to cylinders, vesicles and lamellae, depending on the strength of the enthalpic interaction between the matrix and the block copolymer segments. Selective staining of the PMMA block at the interphase in blends containing SANs was possible only for SANs of higher AN content. This is interpreted as an indication of interfacial microsegregation of the PMMA block from the SAN matrix as the AN content increases. These morphological changes can be explained by differences in the relative solubility of matrix polymer in the micellar corona, which are controlled by the balance between attractive and repulsive interactions with the miscible and immiscible blocks.

(Keywords: block copolymer; blend; morphology; enthalpic interaction; film; transmission electron microscopy)

INTRODUCTION

Homopolymer/block or homopolymer/graft copolymer blend systems are of substantial interest because of the emulsification or compatibilization effect of the block or graft copolymers on immiscible polymers. Many previous studies[1–6] have dealt with blends of a block copolymer with homopolymers. Most of these investigations involved a block copolymer (AB) and a homopolymer (A) having a repeat unit identical with one or more of the copolymer segments. In particular, Thomas *et al.*[3–5] have reported a comprehensive analysis of the role of compositional and structural parameters on the morphology of polystyrene/poly(styrene-*b*-butadiene) and polystyrene/poly(styrene-*b*-isoprene) diblock copolymer blends. In this system[1–6], it is clear that the degree of solubilization of homopolymer in the compatible block copolymer segment is strongly influenced by the molecular-weight ratio (M_H/M_A) of homopolymer (M_H) to the compatible copolymer segment (M_A), and that significant solubilization is possible only when M_H/M_A is of the order unity or less. The thermodynamic origin of the molecular-weight dependence of homopolymer solubility is the loss in configurational entropy due to localization at the interface. At low copolymer volume fraction, decrease of copolymer molecular weight leads to morphological transformations from spherical to cylindrical micelles, and then to vesicles[3–5]. For systems with substantial coronal solubilization, increase of copolymer volume fraction produces a variety of ordered morphologies[1–6]. Morphological studies have also been performed on the blend systems polystyrene/poly(styrene-*b*-methyl methacrylate)[7] and polystyrene/poly(styrene-*b*-methyl methacrylate)/poly(methyl methacrylate)[8]. In addition to the dispersed micellar structures reported by Thomas *et al.*[3–5], micelle aggregation was observed when phase separation occurred at lower temperatures[7]. Also a distinct morphological organization was reported at low microphase volume fractions consisting of reverse micelle formation within large domains of the disperse phase[7,8]. Note that the monomer–monomer segregation tendency is strong in the styrene/isoprene and styrene/butadiene blends[3,9] and weaker in the styrene/methacrylate systems[10].

A theoretical interpretation of the effect of diblock copolymer (AB) on the interfacial tension of blends of homopolymers A and B has been described by Noolandi and Hong[11]. The results indicate[11] that the lowering of interfacial tension is enhanced by an increase in the Flory interaction parameter χ_{AB}, i.e. in the degree of incompatibility of A and B. This is consistent with the

0032-3861/92/173582-11

expectation that the interfacial tension is also determined by the gain in interaction energy when the block copolymer locates at the interface. Also, a theoretical analysis[12] of the degree of mixing of a homopolymer A in the corona of dispersed AB block copolymer micelles, and its consequences for the micellar morphology, has been reported. In the strong segregation limit, a decrease in coronal solubility, and hence a transformation from spherical to cylindrical micellar morphology, is predicted[12] when χ_{AB} increases, or M_{AB}/M_A decreases, or when the fraction of the B block is increased.

Comparatively few morphological studies have been performed on blends[13–17] of block copolymer with homopolymers that are chemically different from each of the copolymer segments but miscible with at least one of them. In such systems, we can expect the exothermic enthalpy of mixing to be an additional thermodynamic driving force for coronal solubilization. Tucker *et al.*[14–17] examined this enthalpic effect on the solubilization of styrene/butadiene/styrene triblock copolymers (SBS) with poly(phenylene oxide) (PPO), which is miscible with PS. They estimated the degree of solubility of homopolymer (PPO) with the PS block copolymer segment by d.s.c. measurement of the glass transition temperature. These experiments confirm that PPO is miscible with the block copolymer PS segment and indicate that the homopolymer solubility is increased in the case of PPO/SBS compared to that[14] of PS/SBS. Their results show that the solubility is strongly enhanced by the favourable enthalpic interaction between homopolymer and block copolymer segment. In particular, it is possible[17] to obtain good solubility when M_H/M_A is substantially larger than unity.

The interfacial tension of blend systems containing homopolymers A and B with a block copolymer (XY) whose segments are chemically different from A and B has been theoretically considered by Vilgis and Noolandi[18], and depends in a complex way on the interaction parameters between all binary pairs. Again, however, the driving force for interfacial activity arises primarily from a gain in interaction energy due to moving the diblock copolymer from the bulk to the interface, offset by a loss in configurational entropy due to localization at the interface.

Clearly it is of interest to investigate the morphological changes induced by systematically varying the enthalpic interaction between the homopolymer and the corresponding block copolymer segment in such blends. It is well known[19] that poly(methyl methacrylate) (PMMA) is miscible with styrene/acrylonitrile copolymers (SAN) having compositions ranging from about 8% acrylonitrile (AN) to about 33% AN. In particular, Fowler *et al.*[20] deduced from miscibility data that the Flory interaction parameter of the PMMA/SAN system has negative values at AN contents between 9.5% and 33%, and exhibits a shallow minimum near 15% AN.

In blends containing SAN polymers and a block copolymer that has PMMA as one component, it follows that the enthalpic interaction between homopolymer and block copolymer can be varied by modifying the AN content. Such systems can be used to examine the effect of the enthalpic interaction on the properties of blends of homopolymers and block copolymer. In this study, we focus on the morphological effect of an enthalpic interaction between the homopolymer and the block copolymer segment. We specifically address the question of whether the morphology is influenced by differences in the degree of coronal solubilization, derived from different interaction strengths.

MATERIALS AND EXPERIMENTAL PROCEDURES

Table 1 lists physical information on the homopolymers used in this study. Note that, for semantic reasons, we refer to the random SAN copolymers as SAN homopolymer. The methyl methacrylate–styrene diblock copolymer, P(S-*b*-MMA), was lot no. SM003, purchased from Polymer Laboratories Inc. and used without further purification. The weight-average molecular weight and polydispersity were reported to be 305×10^3 and 1.08. We determined that this block copolymer has 60 wt% PS and 40 wt% PMMA, on the basis of n.m.r. analysis.

Blends of the desired proportion were prepared by making solutions containing 3% by weight of total polymer in methyl ethyl ketone (MEK). Although the solvent evaporation rate during the casting procedure was very slow (5 days to 1 week), there is always the possibility that the morphology measured in solvent-cast films is not the equilibrium structure[2]. Thus, the chemical characteristics of the solvent may influence the morphology of the cast film by producing a different distribution of solvent in each polymer phase[2]. Although we have no data on the distribution of MEK between SANs, PMMA and PS during the casting process, we can estimate the tendency for solvent distribution by comparing the solubility parameters of polymers and solvent. The solubility parameter of MEK is 9.3 cal cm^{-3}, while those of PS and PMMA are 9.1 and 9.3 cal cm^{-3},

Table 1 Characteristics of the matrix polymers

Abbreviation[a]	Acrylonitrile content (%)[b]	M_w ($\times 10^3$)[c]	M_w/M_n[c]	M_H/M_B[d]	Density[e] (g cm^{-3})
PMMA	–	80	2.06	0.66	1.190
PS	–	61	1.03	0.33	1.047
SAN16	15.5	173	2.12	1.42	1.063
SAN25	24.6	148	2.16	1.21	1.073
SAN29	28.8	141	2.23	1.16	1.078
SAN33	32.8	102	1.95	0.84	1.082

[a] Sources: PMMA, Scientific Polymer Products Inc.; PS, Polysciences Inc.; SAN, Mitsui Toatsu Chemicals Inc.
[b] Determined by i.r.
[c] Determined by g.p.c. (PS standard)
[d] M_w of homopolymer/M_w of compatible block copolymer segment
[e] Estimated by (% PS)ρ_{PS} + (% AN)ρ_{AN}

respectively. Thus we expect that the solvent distribution between PS and PMMA is rather similar. The solubility parameters of SANs depend on the AN content. Since the solubility parameter of polyacrylonitrile is 15.4 cal cm^{-3}, SAN16 has a solubility parameter higher (10.11 cal cm^{-3}) than that of PS but lower than that of SAN33 (11.2 cal cm^{-3}). However, as noted below, since we find that the morphology of SAN33 blends is similar to that of PMMA even though their affinity for MEK is quite different, we feel that solvent distribution effects are not significant in this study. The compositions of the blends prepared in this study are given on a weight-fraction and volume-fraction basis in *Table 2*. Note that we have selected three blend compositions, in each of which polystyrene is the minor component. These are binary blends, which have a weight ratio (weight homopolymer)/(weight block copolymer) = 50/50. We also examined ternary blends with ratios (weight homopolymer)/(weight block copolymer)/(weight PS) = 77.5/15/7.5 and 82/6/12, respectively. The polymer solutions were cast on mercury and the solvent was slowly evaporated at room temperature for 5 days to 1 week. Final solvent removal was accomplished in a vacuum oven at 70°C for 1 day. Thickness of the cast films was about 0.1 mm and the centre of the film was used for TEM measurements.

The casting films were embedded in epoxy resin for electron microscope measurement. The embedded samples were mounted, trimmed and then sectioned to about 50 nm with a Reichert Ultracut N microtome (Reichert-Nissei Inc.). The sections were transferred to a copper or gold grid and selective staining for polystyrene was performed for 1 h at room temperature in ruthenium tetroxide vapour.

Selective staining of the PMMA block copolymer segment was attempted using consecutive treatments with hydrazine and osmium tetroxide[21]. The precise details of the staining procedure were as follows. The microtomed sample was mounted on a gold or copper grid and that grid was covered with a second folding-type grid. The covered sample was dried *in vacuo* at 60°C for 24 h to remove completely any remaining solvent and was then treated with anhydrous hydrazine (Fisher Scientific Inc.) at 60°C for 24 h. The treated sample was washed with distilled water and dried *in vacuo* at 60°C for 24 h to remove the unreacted hydrazine and finally treated with osmium tetroxide (1 wt%) at 60°C for 1 h. Transmission electron micrographs were obtained on JEOL 100-SX and Hitachi H-300 electron microscopes.

RESULTS

Homopolymer/block copolymer blend systems

Figures 1a and *1b* show the TEM micrographs of the neat block copolymer and a 50/50 blend of block copolymer with the poly(methyl methacrylate) homopolymer. In *Figures 2a–d* we exhibit the TEM micrographs of the 50/50 blends of block copolymer with the four SAN copolymers. The dark regions in the TEM photographs are PS, since ruthenium tetroxide stains PS, partially stains SAN (depending on the styrene content) and does not stain PMMA. The block copolymer (*Figure 1a*) shows lamellar domains, which is consistent with expectation[3–5] based on the specified composition (PS/PMMA = 60/40). Also, we note that the long spacing observed in our micrographs

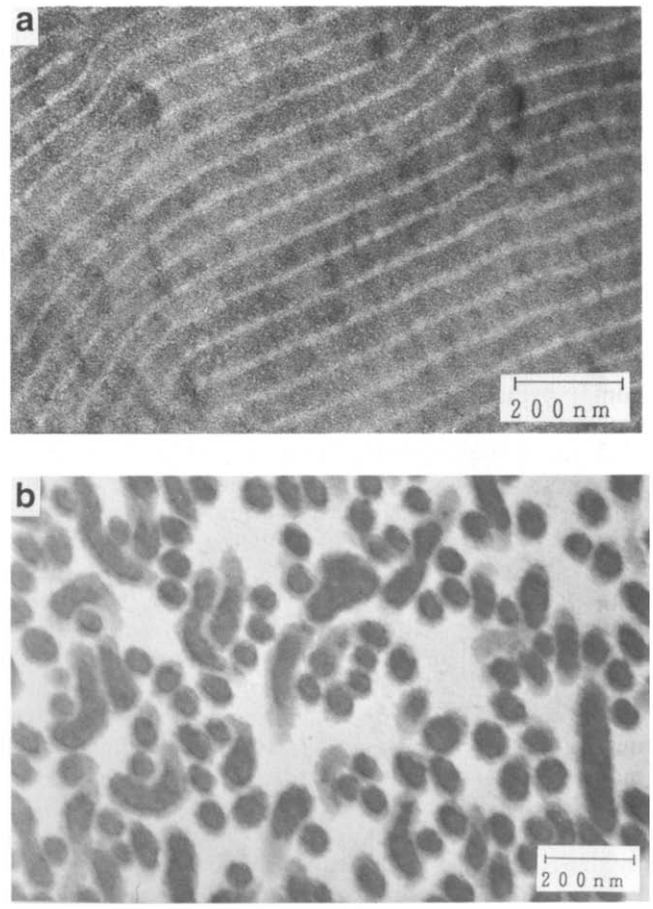

Figure 1 Electron micrographs of: (a) the neat P(S-*b*-MMA) block copolymer; (b) a 50/50 blend of P(S-*b*-MMA) with PMMA

(66 ± 12 nm) is numerically comparable to that (74 nm) computed from a relation $d = 1.35N^{1/2}$ determined by small-angle X-ray scattering for 50/50 P(S-*b*-PMMA) block copolymers[10]. In the 50/50 blends, the lamellar morphology of the block copolymer changes to disperse spheres or a disordered cylinder structure or a mixture of the two. This clearly shows that each homopolymer solvates the PMMA segment of the block copolymer. First we note that the micrographs of the SAN16/block copolymer blends are not very distinct because of the small domain sizes and the similar RuO_4 staining of SAN16 and PS. However, it appears that the morphology of this blend consists of relatively uniform spherical domains (*Figure 2a*). The corresponding blends with SAN25 (*Figure 2b*), SAN29 (*Figure 2c*) and SAN33 (*Figure 2d*) exhibit predominantly spheres with some elongated structures that appear similar to cylindrical domains. When the homopolymer is PMMA (A/AB system), the morphology (*Figure 1b*) clearly is that of disordered spheres and cylinders, predominantly cylinders. In a 70/30 PMMA/block copolymer blend, not shown, we found predominantly spheres. We note that our observations on the PMMA/block copolymer blend are consistent with the experimental results of Lowenhaupt and Hellmann[7], who also report a dispersed micellar morphology at these volume fractions.

Homopolymer/block copoiymer/homopolystyrene (PS) blend systems

Figures 3 and *4* show the TEM micrographs of the ternary blends containing homopolymer/block

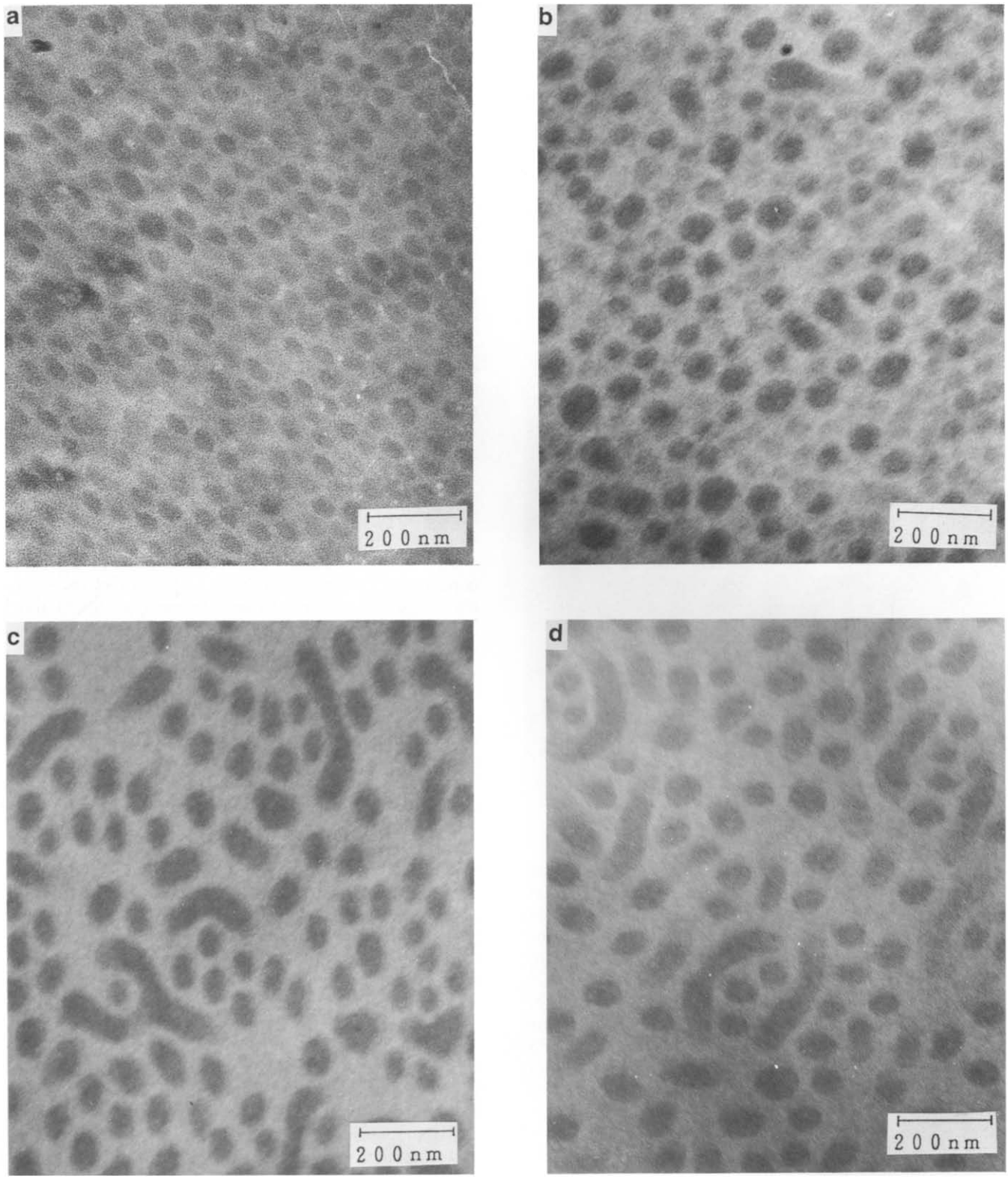

Figure 2 Electron micrographs of 50/50 blends of P(S-*b*-MMA) with: (a) SAN16; (b) SAN25; (c) SAN29; (d) SAN33

copolymer/PS at a composition ratio 77.5/15/7.5. The results demonstrate that in each blend the PS homopolymer dissolves in the PS segment of the block copolymer. The morphology exhibited by the PMMA/block copolymer/PS blend consists predominantly of disordered lamellae with some vesicles (*Figure 3*). We point out that Kinning *et al.*[5] observed a transition to a vesicular morphology in blends of polystyrene with poly(styrene-*b*-butadiene), P(S-*b*-B), when the solubility of PS in the micelle corona is sufficiently reduced. Thus we believe that the lamellar morphology in our 77.5/15/7.5 PMMA/P(S-*b*-MMA)/PS blend is consistent with the greater interfacial solubility of the matrix polystyrene ($M_H/M_A = 0.33$) compared to that of the matrix PMMA ($M_H/M_B = 0.62$). We note further that lamellar structures were also observed by Lowenhaupt and Hellmann[8] in symmetrical PS/P(S-*b*-MMA)/PMMA blends when the weight fraction of block copolymer

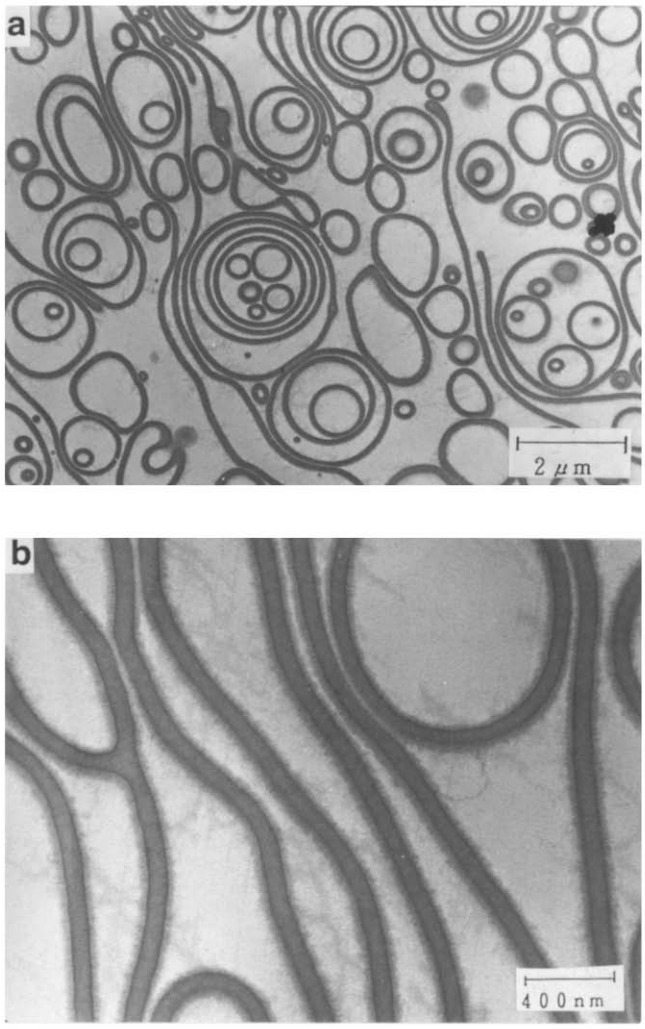

Figure 3 Electron micrographs of 77.5/15/7.5 blends of SAN/P(S-*b*-MMA)/PS: (a) low resolution; (b) high resolution

$f > 0.2$. By contrast, however, the styrene microphase in the SAN25/block copolymer/PS blend (*Figure 4b*) has spherical domains similar to those in the SAN16/block copolymer (50/50) blend (*Figure 2a*), but the size of the spherical PS inclusions increases (from about 60 nm to about 120 nm). The SAN16/block copolymer/PS blend has (*Figure 4a*) almost the same morphology as that of the SAN25 ternary blend but in addition shows some vesicular domains. The SAN29/block copolymer/PS blend (*Figure 4c*) shows a mixture of spheres and a multilamellar vesicle morphology. The multilamellar vesicle morphology becomes dominant in the SAN33/block copolymer/PS (*Figure 4d*).

TEM studies were also performed on ternary blends of homopolymer/block copolymer/PS at composition 82/6/12. In this case, SAN16, SAN33 and PMMA were used as the homopolymers. The SAN16/block copolymer/PS again exhibits predominantly spherical domain morphology with a few vesicular structures as observed in the 77.5/15/7.5 blend (*Figure 5a*). However, the PS domain size increases to 250 nm, reflecting further micellar solubilization of homopolystyrene. On the other hand, low-magnification TEM photographs show that the SAN33/block copolymer/PS and PMMA/block copolymer/PS blends have a completely different morphology. Large (1 to 10 μm) strongly stained domains are found dispersed in a SAN33 or a PMMA matrix and each domain has some internal microstructure. The large domains enclose many unstained small particles (about 50 to 200 nm), which can be seen at high magnification (*Figures 5b* and *5c*). This latter behaviour appears similar to that reported by Lowenhaupt and Hellmann[7,8] at low copolymer volume fractions in the PS/P(S-*b*-MMA)/PMMA system, and represents a combination of macrophase followed by microphase separation. Thus the small inclusions are considered to be the pure PMMA segment of the block copolymer or a mixture of the PMMA segments with the co-mixing homopolymer (SAN33 or PMMA).

Selective staining of the PMMA block copolymer segment

It is of interest to attempt to characterize the spatial distribution of the block copolymer at the interfacial zones in these multicomponent blends. To do this we attempted selective staining of the PMMA corona. This effort was, however, limited to partial success since we were able to stain only binary blends containing SAN33 and ternary blends containing SAN29 and SAN33. Since we can achieve staining of the PMMA segment in the neat block copolymer and in the presence of SANs of high AN content, we infer that the ease of staining reflects variations in the interfacial concentration of PMMA.

Figure 6 shows the TEM photographs of the block copolymer (*Table 6a*), the binary SAN33/block copolymer blend (50/50) (*Figure 6b*) and the ternary SAN33/block copolymer/PS blend (77.5/15/7.5) (*Figure 6c*) stained with hydrazine–osmium tetroxide. The TEM photograph of the block copolymer (*Figure 6a*) shows the lamellar domain structure also evident in *Figure 1a*, but the staining of each domain is reversed relative to that of ruthenium tetroxide staining. This observation confirms that PMMA can be selectively stained by the hydrazine–osmium tetroxide method. The SAN33/block copolymer (50/50) blend has spherical or cylindrical micellar domain morphology (*Figure 2d*) while the SAN33/block copolymer/PS (77.5/15/7.5) blend has a multilamellar type domain structure (*Figure 4d*). These blends, on staining with hydrazine–osmium tetroxide (*Figures 6b* and *6d*), show, respectively, ring-like and lamellar stained regions, which closely follow the outlines of the microdomains apparent in these blends when stained with ruthenium tetroxide. It is of further interest to remark that the width of the PMMA staining (7.5 ± 1.5 nm) is smaller than the r.m.s. end-to-end distance of a Gaussian PMMA chain of $M_w = 122\,000$ (22 ± 2.5 nm). Our observations are consistent with the idea[11,18] of a concentration gradient of PMMA extending from the interface towards the SAN phase. With increasing AN content of the SAN, the interfacial concentration of PMMA rises because of increased repulsion between the PS and SAN. Consequently, a PMMA-rich region is formed close to the interface in the SAN33 blends, and it is this which shows staining. Conversely, in the SAN16 and SAN25 blends, the PMMA block extends into the SAN matrix and the coronal PMMA concentration is too low to enable staining.

DISCUSSION

The molecular origin of the morphological transitions that occur in block copolymer/solvent systems as a function of the relative volume fraction of the

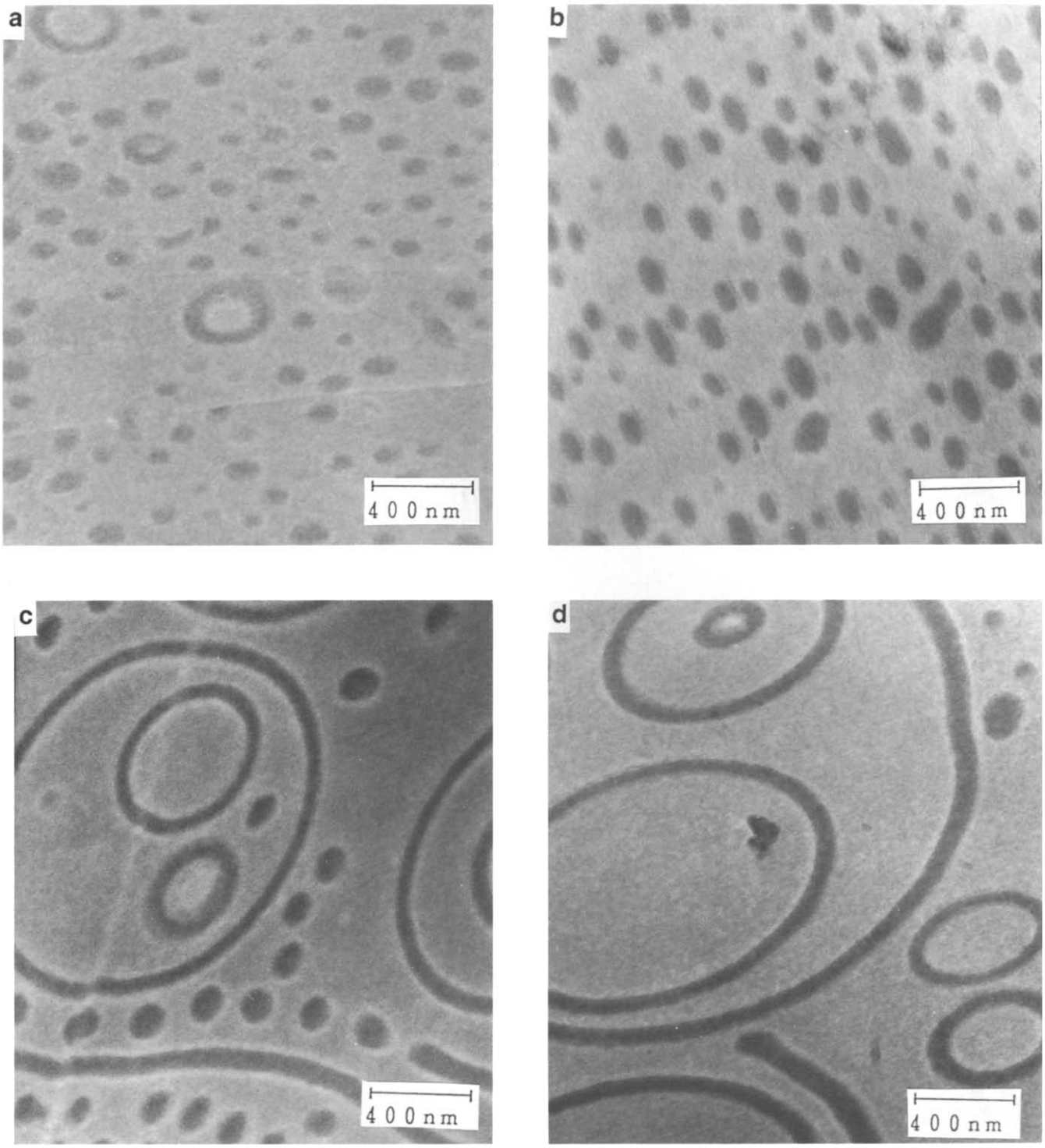

Figure 4 Electron micrographs of 77.5/15/7.5 blends of SAN/P(S-*b*-MMA)/PS: (a) SAN16; (b) SAN25; (c) SAN29; (d) SAN33

microphases has been[22,23] examined experimentally and theoretically. These transformations can be intuitively understood[22,23] in terms of the interface curvature and the packing requirements of the blocks in the domain space. Similar arguments are used[24] to predict whether amphiphilic surfactants will assemble into spherical or cylindrical micelles or bilayers from a consideration of their head-group area and hydrocarbon chain volume.

Thomas and coworkers[3–5] have identified such morphological transitions in blends of polystyrene and styrene/butadiene (SB) or styrene/isoprene (SI) diblock copolymers as a function of the PS volume per cent and the relative molecular weight of the PS homopolymer and the PS segment of the block copolymer. It is well known that the degree of solubilization of the homopolymer to the corresponding block copolymer segment is strongly influenced by their molecular-weight ratio and that lower-molecular-weight homopolymers are more miscible with the block copolymer segment. Using electron microscopy and small-angle X-ray scattering experiments, Kinning *et al.*[4,5] concluded that the morphological changes in the PS/SB system could be interpreted in terms of the general relationships discussed by Sadron and Gallot[22] relating domain

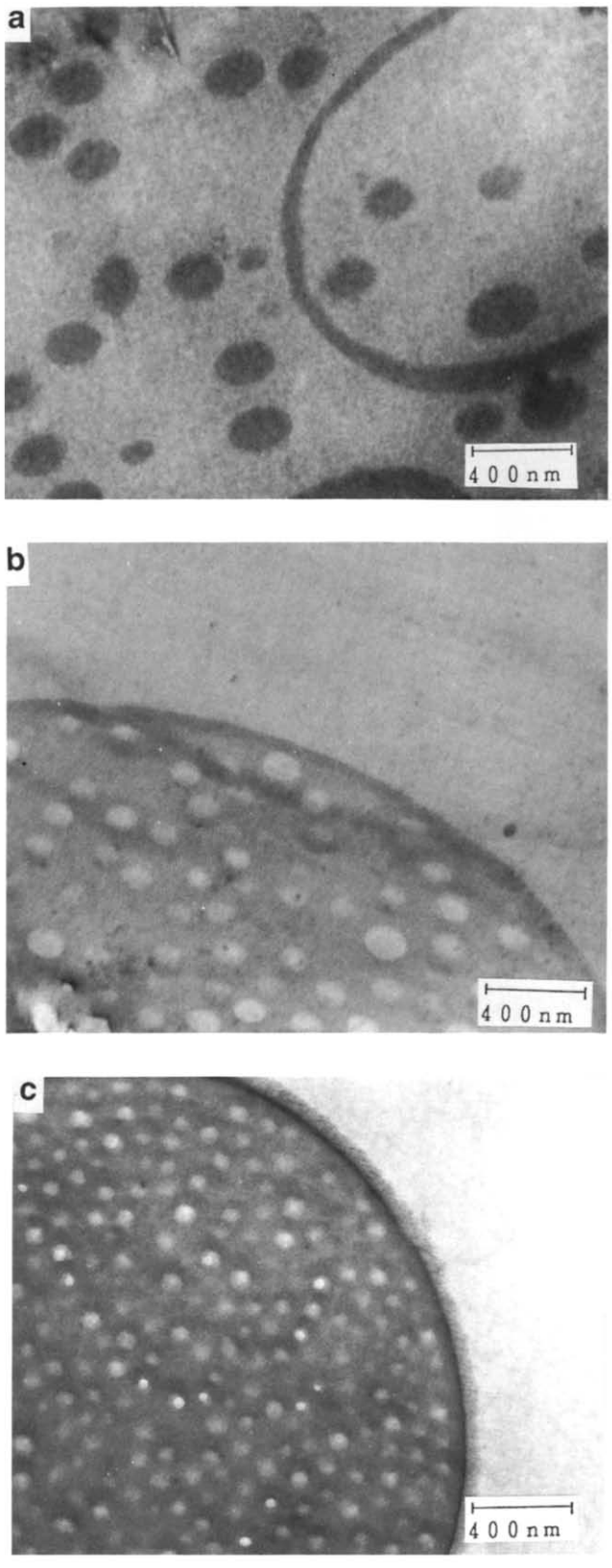

Figure 5 Electron micrographs of 82/6/12 blends of: (a) SAN16/P(S-*b*-MMA)/PS; (b) SAN33/P(*b*-MMA)/PS; (c) PMMA/P(S-*b*-MMA)/PS

morphology to the relative microphase volume fractions in block copolymer/solvent systems.

Similar factors are relevant to our blend systems. However, we are more interested here in discussing the morphological differences between systems that have (essentially) the same microphase volume fractions, ϕ_{SAN}, ϕ_{PS} and ϕ_{PMMA}, as shown in *Table 2*. There is only limited theoretical work on the degree of solubilization of homopolymers with chemically distinct block copolymer segments. Tucker and Paul[17] describe a simple model for estimating the enthalpic contributions in homopolymer/block copolymer blends and showed that these effects significantly increased the degree of interfacial solubilization compared with the case where there is only an entropic mixing effect. Their analysis is limited to the situation in which the blends exhibit a lamellar structure in which both domains are connected by a block

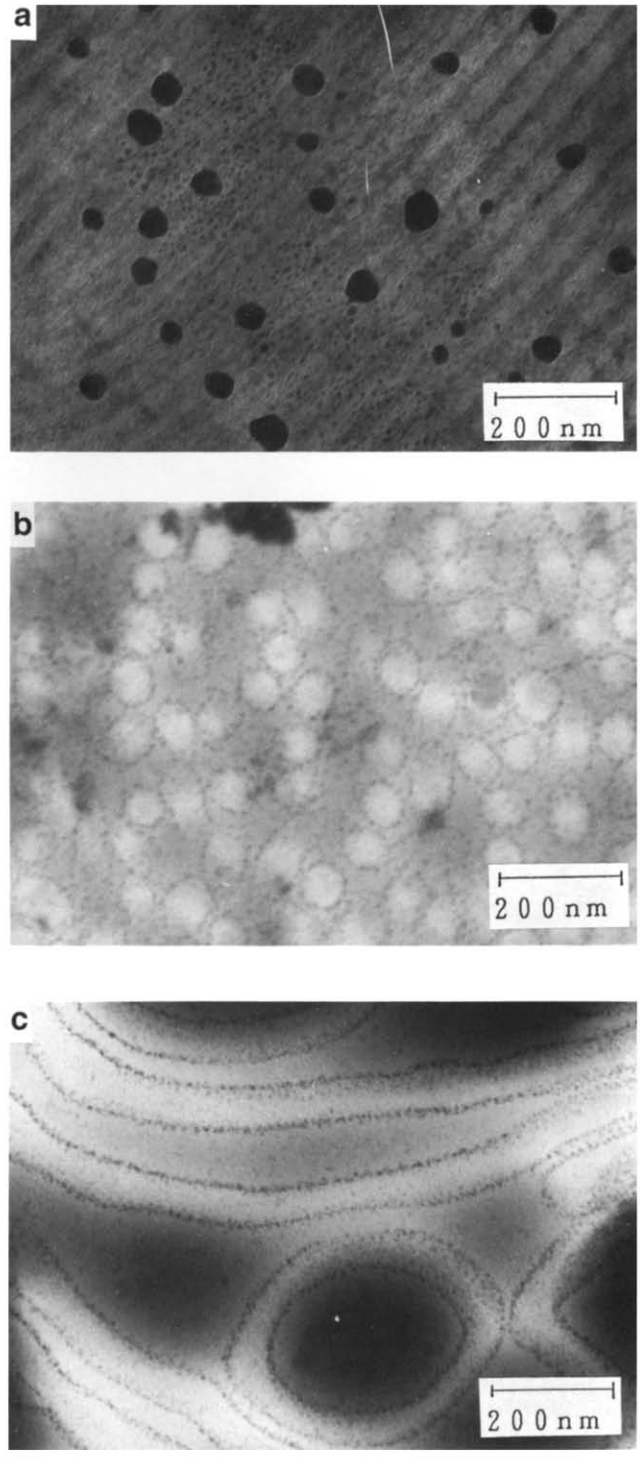

Figure 6 Staining of PMMA by hydrazine–OsO_4 treatment: (a) neat P(S-*b*-MMA) block copolymer; (b) 50/50 blend of SAN33/P(S-*b*-MMA); (c) 77.5/15/7.5 blend of SAN33/P(S-*b*-MMA)/PS

Table 2 Calculated heats of random mixing

(a) ΔH_{mix} (50/50 blends)

Matrix	$B_{(SAN/MMA)}$ (cal cm^{-3})	$B_{(SAN/Sty)}$ (cal cm^{-3})	ϕ_{SAN}	ϕ_{PS}	ϕ_{PMMA}	ΔH_{mix} (cal cm^{-3})
PMMA			–	0.328	0.672	0.040
SAN16	−0.081	0.133	0.508	0.310	0.182	0.024
SAN25	−0.11	0.342	0.506	0.311	0.183	0.056
SAN29	−0.091	0.473	0.505	0.312	0.183	0.076
SAN33	−0.052	0.619	0.504	0.313	0.183	0.103

(b) ΔH_{mix} (77.5/15/7.5 blends)

	ϕ_{PS}	ϕ_{PMMA}	ϕ_{SAN}	ΔH_{mix} (cal cm^{-3})
PMMA	0.183	0.83	–	0.025
SAN16	0.168	0.052	0.778	0.016
SAN25	0.169	0.052	0.778	0.042
SAN29	0.170	0.052	0.778	0.060
SAN33	0.170	0.052	0.778	0.081

(c) ΔH_{mix} (82/6/12 blend)

	ϕ_{PS}	ϕ_{PMMA}	ϕ_{SAN}	ΔH_{mix} (cal cm^{-3})
PMMA	0.174	0.83	–	0.026
SAN16	0.158	0.0212	0.811	0.016
SAN33	0.161	0.0212	0.811	0.080

copolymer segment. This model cannot be adapted quantitatively to our system, which contains large amounts of homopolymer. However, the theoretical model and the accompanying experimental studies of blends of poly(phenylene oxide) and a styrenic block copolymer clearly show[16,17] that enthalpic effects increase the degree of coronal solubilization and thus a similar behaviour can be expected in our systems. Also, these authors note[17] that morphological transitions will modify the coronal solubility of the homopolymer. In particular, the entropic penalty for dissolving homopolymer is decreased in changing from spheres to cylinders to lamellae. We further comment that Tucker *et al.*[14–17] determined the degree of solubilization of the PPO homopolymer in the PS microphases of the triblock copolymer by differential scanning calorimetry (d.s.c.). Unfortunately, in our system, we cannot use this method because the T_g of PS, PMMA and the SANs are almost equal. However, it is clear that observation of the morphological transitions described above provides alternative evidence for increased solubilization by enthalpic interactions. Also pertinent to our discussion is the theoretical description of interfacial tension in the system A(X-*b*-Y)/B by Vilgis and Noolandi[18]. For the symmetrical blend, when $\chi_{AB} = \chi_{AX} = \chi_{BY} = \chi_{XY} = \chi_1$ and $\chi_{AY} = \chi_{BX} = \chi_2 > \chi_1 > 0$, these authors showed that the interfacial tension lowering is strongly enhanced by increase of the repulsion between the homopolymer and the immiscible copolymer segment.

In general, therefore, we must consider three factors:

(1) The change in volume and configurational entropy on mixing of the different polymers.

(2) The enthalpic interaction between the matrix homopolymer(s) and the immiscible block copolymer segment.

(3) The enthalpic interaction between the matrix homopolymer(s) and the miscible block copolymer segment.

In many miscible polymer blends, there is a negative volume change on mixing. In blends of SAN (18% AN) and PMMA, however, Naito *et al.*[25] showed that the volume change on mixing is small. Therefore, as a reasonable approximation, we may use a simple additive rule to estimate the volume of the mixed SAN and PMMA block copolymer segment (*Table 2*).

The configurational entropy of mixing of homopolymer with block copolymer segment decreases with increase in the ratio, M_H/M_A, of molecular weights[3–6]. Thus, the entropy penalty for PMMA will be smaller than that of the SANs (*Table 1*). Since the morphological evidence indicates that the PS/PMMA block copolymer is a more effective compatibilizer for the SANs than for PMMA, it seems clear that the dominant role is played by the enthalpic contributions. Note also in this regard that the morphological differences observed when comparing blends containing SANs of differing AN content are in the direction opposite to that expected on the basis of M_H/M_A ratio. Specifically for SANs of higher AN content, a decrease in M_H/M_A (*Table 1*) would lead[3–6] to an increase in coronal solubility of homopolymer, i.e. a morphological change from lamellae to spheres, opposite to what is observed.

The interaction parameters of our PS/SAN blends are estimated to be comparable to those of PS/PMMA even when the SAN has a comparatively small AN content (i.e. 16%), because of the great differences in the binary interaction parameters of styrene/acrylonitrile (S/AN) and styrene/methacrylate (S/MMA)[26]. In *Table 2*, we list the binary energy density interaction parameters for the copolymers computed using the reported values of Nishimoto *et al.*[26]: $B(AN/MMA) = 4.11$ cal cm^{-3}, $B(S/AN) = 6.74$ cal cm^{-3}, $B(S/MMA) = 0.181$ cal cm^{-3}. Thus we estimate a binary interaction parameter for PS/SAN16 of 0.133 cal cm^{-3}, and larger values for higher AN content. Based on *Table 2*, we expect a stronger repulsion between the SANs of higher AN

content and the PS segment compared to PS/PMMA (0.181 cal cm^{-3}). This analysis lends support to the possibility that a thin, SAN-depleted PMMA phase exists near the interface between the PS segment and the SAN29 and SAN33 homopolymers in this blend system, as suggested by the hydrazine–OsO_4 staining (*Figure 4*).

The enthalpic interaction between the SANs and the PMMA segment of the block copolymer also depends on the AN content. Theoretical evaluation indicates[26] that, for AN content in the range 10–33%, $B(\text{SAN/MMA}) \leqslant 0$, indicating a favourable exothermic interaction, and for our blends we find that this interaction lies in the order SAN25 < SAN29 < SAN16 < SAN33 < 0 as shown in *Table 2*. By contrast, the interaction between the PMMA homopolymer and the PMMA block copolymer segment must be zero. For reference, we also show in *Table 2* the computed random heat of mixing for each blend. As expected, all systems are endothermic (*Table 2*), with the SAN16 blends showing the smallest ΔH_{mix}. The gain in interaction energy when the block copolymer locates at the interface provides a large driving force for all blends.

Considering first the 50/50 binary blends, the morphological evidence (*Figures 1* and *2*) suggests that the PS/PMMA block copolymer is a better emulsifier for blends of PS with all four SAN copolymers than for blends of PS with PMMA since the disperse phases of the former have predominantly small spherical micelles in contrast to the preponderance of cylindrical micelles in the latter. Based on the above discussion, we assign this result to the enhanced exothermic solubilization of the SAN matrix by the PMMA corona of the micelles. It is pertinent to note in this regard that, consistent with the observations of Tucker *et al.*[17] for the SBS/PPO system, we find excellent emulsifying effect, and hence substantial coronal solubility of SANs when $M_H/M_A > 1.0$. In comparing the morphologies of the different SAN blends (*Figure 2*), it is evident that those of the SAN16 and SAN25 blends consist almost entirely of spherical micelles whereas the SAN29 and SAN33 blends contain significant numbers of elongated structures (cylinders or ellipses). We infer that this effect arises because of the increased repulsion between the PS micellar core and the SAN matrix at higher AN content, resulting in a decrease in coronal solubility of SAN. Note that this suggestion is consistent with our observation that the PMMA block of the micellar corona can be stained only in the SAN33 blend (*Figure 3*). In any event, it is apparent that the micellar morphology is strongly influenced by the net enthalpic interaction of the matrix homopolymer with the micellar core and corona.

In the ternary blends of SAN/block copolymer/PS = 77.5/15/7.5, the morphology exhibits rather larger systematic changes (*Figure 4*) from predominantly spherical micelles (SAN16 and SAN25) to a mixed micellar–vesicular morphology (SAN29 and SAN33). In comparison, the PMMA/block copolymer/PS blend has a mixed vesicular–lamellar morphology (*Figure 3*). Again, we can neglect the relatively small changes in volume fraction between the systems and conclude that these results clearly demonstrate the effectiveness of the SAN–MMA enthalpic interaction in increasing the degree of matrix solubilization. We point out, as evident in *Table 2*, that ternary blends containing SAN33 or PMMA in the ratio homo/block/PS = 77.5/15/7.5 have a smaller volume fraction of the disperse styrene phase, ϕ_{PS}, than that of the binary 50/50 blends of SAN33/block copolymer. Ordinarily, we expect that a decrease of ϕ_{PS} will tend to change the morphology from lamellae to spheres. However, we note (*Table 1*) that the molecular-weight ratio (M_H/M_B) for the PS homopolymer ($M_H/M_B = 0.33$) is substantially smaller than that for the PMMA homopolymer ($M_H/M_B = 0.66$) and for the SAN33 copolymer ($M_H/M_B = 0.84$). As is well known, the degree of coronal solubilization depends principally on the relative molecular weight when the enthalpic effect is small[1–6]. Thus, in the above blends, we may expect the solubility of the PS homopolymer in the PS block segment to be much larger than that of PMMA or SAN33 in the PMMA block segment. It follows that it is the interfacial compositional heterogeneity, enriched in homopolystyrene, that determines the transition to a lamellar morphology in the ternary blends containing PMMA, SAN29 and SAN33.

As for the binary systems, the morphological evidence for the ternary blends indicates that the block copolymer is a more effective emulsifier for PS and the SAN copolymers than for PS and PMMA. Again, this can be attributed to the enhanced solubilizing power of the PMMA segment for the SAN matrix. To explain the substantial variation in emulsifying effect in the blends containing SAN, which falls in the order SAN25 $\gtrsim$ SAN16 > SAN29 > SAN33, we must invoke the increased repulsion between the PS core and the SANs of higher AN content (cf. *Table 2*). This effect appears to be enhanced in the ternary compared to the binary blends, as evidenced by more dramatic changes in morphology, and by the fact that PMMA staining of the interface can be accomplished for both the SAN29 and SAN33 blends. This is presumably because of the penetration of the interface by the mobile low-molecular-weight PS, which results in a more effective repulsion of the SANs.

Comparing the 77.5/15/5 and 82/6/12 homopolymer/block copolymer/PS ternary blends, these have essentially the same volume fraction of the styrenic disperse phase (*Table 2*), but differ in the relative concentration of homopolymers to block copolymer. This has only a minor effect on the morphology of the SAN16/block copolymer/PS blend, which is essentially the same as the SAN16 blends of other composition (dispersed spheres) (*Figure 5a*). In the SAN33 or PMMA/block copolymer/PS systems, however, the block copolymer and the PS homopolymer form a quite different morphology similar to that observed by Lowenhaupt and Hellmann[7], consisting of large macrophase-separated domains that contain some of the SAN33 and PMMA as small inclusions (*Figures 5b* and *5c*). These domains are dispersed in a SAN33 or PMMA matrix. The internal concentration modulation observed in the domains in the PMMA blend occurs on a smaller length scale than that in the SAN blend, and resembles the micellar aggregation reported by Lowenhaupt and Hellmann[7]. These distinctive morphologies are interpreted[8] as due to a two-step kinetic process consisting of initial macrophase separation of polystyrene-rich domains accompanied by internal microphase separation. It is somewhat surprising, in view of the large PS–SAN33 repulsion and weak PMMA–SAN33 attraction, that the PS-rich domains in the SAN33 blend clearly contain quantities of included SAN33 in addition to block copolymer. This may represent kinetically trapped

SAN33 (cf. the larger molecular weight of SAN33 relative to PS).

In summary, a comparison of the morphological results for the blends containing PMMA *versus* those containing SANs clearly shows that, in the latter, the solubilization of the homopolymer and compatible block copolymer segment is enhanced by the enthalpic interaction between them and progressively diminished by an increase in the repulsive interaction across the interface. Thus, the emulsifying power of a block copolymer A-*b*-X for blends of immiscible polymers A and B, with A as the minor phase, is increased by a strong exothermic interaction between B and X, provided that the repulsion between A and B is relatively weak. It also appears that the influence on emulsifying ability of the molecular weight of B relative to that of block X is comparatively weak. It would be of interest to investigate the effect of an increase in the repulsion between blocks A and X, and of variation in molecular weight of homopolymer A relative to block A.

Although solvent casting cannot be compared directly with typical commercial mixing processes, e.g. melt blending in extruder and roll-mill, our results motivate some general comments regarding the ability of block copolymers to improve the properties of immiscible polymer blends via emulsification. First, we recall that the degree of coronal solubility of the SANs is larger than that of PMMA even though the relative molecular weight of homopolymer and the compatible block copolymer segment, M_B/M_X, is larger than unity. This supports the conclusions of Tucker *et al.*[17] that relative molecular weight is a less critical factor in blends with a strong enthalpic interaction. Thus it may be possible to use a low-molecular-weight block copolymer, which can still act as an effective compatibilizer and will facilitate reaching a quasi-equilibrium state during the blending process because of its lower viscosity. We note, however, that the emulsifying role of block copolymers in melt blending processes is apparently not as well understood as in solvent blending. For example, in melt blending of polyethylene and polystyrene with a hydrogenated butadiene/styrene block copolymer, Fayt *et al.*[27] report that the matrix to block molecular-weight ratio is less important for compatibilizing effectiveness compared to solvent blending.

Secondly, we observe that the disperse phase sizes of the ternary blends containing SANs are generally smaller than those containing PMMA at comparable compositions. Thus the block copolymer is a better emulsifier in the SAN blends than in the PMMA blends. Bearing in mind that the block copolymer content is higher (15 wt%) than in a typical melt blending application, these results support the idea that a block copolymer with a strong enthalpic interaction will be a more effective compatibilizer. Schwarz *et al.*[28] observed a similar phenomenon in the morphology of blends of high-density polyethylene (HDPE), polystyrene (PS) containing variable amounts of a miscible polyether copolymer (PEC) and a hydrogenated butadiene/styrene block copolymer. PEC is structurally similar to (2,6-dimethyl-1,4-phenylene oxide, PPO), except for a minor (about 5%) trimethylphenol component, and has virtually the same properties as PPO, including complete miscibility with PS over the full range of compositions. Thus PS/PEC blends that have a higher amount of PEC have a higher enthalpic interaction with the PS segment of the block copolymer. It was found that the block copolymer produces a smaller disperse phase size in the HDPE/80PEC blend (80% PEC and 20% PS) than in the HDPE/PS blend.

Thirdly, we find that the enthalpic interaction can increase the amount of homopolymer dissolved in the compatible block copolymer segment. As observed elsewhere[28], this leads to the possibility that the enthalpic interaction will promote better interfacial adhesion between two immiscible homopolymers. We point out, however, that these two potential roles of block copolymer compatibilizers, viz. the emulsifying effect and the promotion of interfacial adhesion, are not necessarily related. For example, as noted earlier, Vilgis and Noolandi[18] deduced theoretically that, in the blend system polymer A/polymer B/block copolymer XY, localization of the block copolymer at the interface and a reduction of interfacial tension will occur even if the segments X and Y are each immiscible with A and B. This occurs when the Flory interaction parameters χ_{AY} and $\chi_{BX} > \chi_{AB}, \chi_{XY}, \chi_{AX}$ and χ_{BX}. However, the interfacial adhesion of such a blend may not be enhanced because of the immiscibility of the homopolymers and block copolymer segments. This suggestion is reinforced by our observations here where we see a microsegregation of the SAN matrix from the PMMA block at higher AN content due to the increased repulsion with the PS block. It is therefore interesting to note that Fayt and Teyssie found[29,30] that a butadiene/methyl methacrylate block copolymer reduced disperse phase sizes and gave improved mechanical properties in blends of SAN27 with an SBS thermoplastic elastomer. On the other hand, a styrene/methyl methacrylate block copolymer has substantially less effect on mechanical properties of the blends although it did give smaller particle sizes[29]. Also, Schwarz *et al.*[28] have reported, when comparing blends of polymers with block copolymer compatibilizers, that certain copolymers produced poorer mechanical properties even though they had a better emulsifying effect. It would be of interest in this connection to compare the mechanical properties of our SAN29 and SAN33 blends, which show interfacial staining of PMMA, with the SAN16 and SAN25 blends, which do not.

In conclusion, we have demonstrated that the enthalpic interaction between homopolymer and block copolymer segment has a significant influence on the morphology of solvent-cast blend films, which supports the concept that variation in the enthalpic interactions offers a strategy for controlling the properties of polymer blends[17,18,28–30]. The morphological data are consistent with the idea that the coronal solubility of the block copolymers and hence the interfacial tension are only weakly dependent on the molecular-weight ratio M_H/M_A, but are strongly influenced by the presence of an exothermic interaction of the block segments with the matrix, and by the repulsive interaction strength across the interface.

ACKNOWLEDGEMENT

This research was made possible by financial support from Mitsui Toatsu Chemicals Inc. and the Edison Polymer Innovation Corporation.

REFERENCES

1 Inoue, T., Soen, T., Hashimoto, T. and Kawai, K. *Macromolecules* 1970, **3**, 87
2 Meier, D. *J. Polym. Prepr. Am. Chem. Soc. Div. Polym. Chem.* 1977, **18**(1), 340
3 Thomas, E. L. and Winey, K. I. *Proc. ACS Div. Polym. Mater. Sci. Eng.* 1990, **62**, 686
4 Kinning, D. J., Thomas, E. L. and Fetters, L. J. *J. Chem. Phys.* 1989, **90**, 5806
5 Kinning, D. J., Winey, K. I. and Thomas, E. L. *Macromolecules* 1988, **21**, 3502
6 Bemey, C. V., Cheng, P. L. and Cohen, R. F. *Macromolecules* 1988, **21**, 2235
7 Lowenhaupt, B. and Hellmann, G. P. *Colloid Polym. Sci.* 1990, **268**, 885
8 Lowenhaupt, B. and Hellmann, G. P. *Polymer* 1991, **32**, 1065
9 Hashimoto, T., Fujimura, T. and Kawai, H. *Macromolecules* 1980, **13**, 1660
10 Coulon, G., Russell, T. P., Deline, V. R. and Green, P. F. *Macromolecules* 1989, **22**, 2581
11 Noolandi, J. and Hong, K. M. *Macromolecules* 1984, **17**, 1531
12 Mayes, A. M. and Olvera de La Cruz, M. *Macromolecules* 1988, **21**, 2543
13 Meyer, G. C. and Tritscher, G. E. *J. Appl. Polym. Sci.* 1978, **22**, 719
14 Tucker, P. S., Barlow, J. W. and Paul, D. R. *J. Appl. Polym. Sci.* 1987, **34**, 1817
15 Tucker, P. S., Barlow, J. W. and Paul, D. R. *Macromolecules* 1988, **21**, 1678
16 Tucker, P. S., Barlow, J. W. and Paul, D. R. *Macromolecules* 1988, **21**, 2794
17 Tucker, P. S., Barlow, J. W. and Paul D. R. *Macromolecules* 1988, **21**, 2801
18 Vilgis, T. A. and Noolandi, J. *Macromolecules* 1990, **23**, 2941
19 Coleman, M. M., Graf, J. F. and Painter, P. C. 'Specific Interactions and Miscibility of Polymer Blends', Technomic, Basel, 1991, Ch. 2, p. 113
20 Fowler, M. E., Barlow, J. W. and Paul, D. R. *Polymer* 1987, **28**, 2145
21 Hamazaki, T., Karchiku, Y., Hada, R. and Izumi, M. *J. Appl. Polym. Sci.* 1977, **21**, 1569
22 Sadron, C. and Gallot, B. *Makromol. Chem.* 1973, **164**, 301
23 Ohta, T. and Kawasaki, K. *Macromolecules* 1986, **19**, 2621
24 Israelachvili, J. N. in 'Physics of Amphiphiles, Micelles, Vesicles and Microemulsions' (Eds. V. Degiorgio and M. Conti), North-Holland, Amsterdam, 1985, p. 24
25 Naito, K., Johnson, G. E., Allara, D. L. and Kwei, T. K. *Macromolecules* 1978, **11**, 1260
26 Nishimoto, M., Keskkula, H. and Paul, D. R. *Polymer* 1989, **30**, 1279
27 Fayt, R., Jerome, R. and Teyssie, Ph. *Makromol. Chem.* 1986, **187**, 837
28 Schwarz, M. C., Barlow, J. W. and Paul, D. R. *J. Appl. Polym. Sci.* 1989, **37**, 403
29 Fayt, R. and Teyssie, Ph. *Macromolecules* 1986, **19**, 2077
30 Fayt, R. and Teyssie, Ph. *Polym. Eng. Sci.* 1989, **29**, 538